

Linear demultiple solution based on the concept of bottom-multiple-generator (BMG) approximation: some new results

Abiola O. Oladeinde* and Luc T. Ikelle

Center for Automated Seismic Processing (CASP), Department of Geology and Geophysics, Texas A&M University, College Station, Texas 77843-3115 USA

Received April 2005, revision accepted January 2006

ABSTRACT

Recent advances in the demultiple technique have shown that a multidimensional convolution of a portion of data containing only primaries with the whole data (containing both primaries and multiples) can allow us to predict and attenuate all orders of free-surface multiples that are relevant for practical purposes. One way of constructing the portion of the data containing only primaries is by muting the actual data just above the first free-surface multiple to arrive. The location of the mute is generally known as the bottom-multiple-generator (BMG) reflector; the portion of the data containing only primaries required for constructing the free-surface multiples is located above the BMG. The outstanding question about this method is how effective can the technique be when the BMG cuts through several seismic events, as is the case in long-offset data or in very complex shallow geology. We present new results which demonstrate the fact that the BMG location may cut through several seismic events without affecting the accuracy or the cost of demultiple.

INTRODUCTION

In a paper published by Ikelle *et al.* (2004), a demultiple technique was proposed. The concept of this technique is to define a portion of the data containing only primaries by muting the data just above the first free-surface multiple to arrive. The location of the mute is also known as the bottom-multiple-generator (BMG) reflector. The multidimensional convolution of the portion of the data containing primaries with the actual data allows us to predict and attenuate all orders of free-surface multiples and therefore solve the problem of demultiple in towed-streamer data. The outstanding question, not demonstrated by the examples presented in the paper, is what happens to demultiple results when the muting at the BMG reflector cuts through several seismic events. Here, we demonstrate that this demultiple technique is effective when the BMG cuts through several seismic events, by applying the technique to a synthetic data set generated from a complex shallow ge-

ology (see Fig. 1) using the elastic finite-difference modelling technique. Before we give the details of our demonstration, we first review the demultiple technique as described by Ikelle *et al.* (2004).

The demultiple technique can be described as a two-step process. We denote the two components of towed-streamer data without the direct-wave arrivals by $\Phi_0 = \{P_0, V_0\}$, where P_0 is the pressure data and V_0 is the vertical particle velocity, and we denote the portion of towed-streamer data above the BMG reflector by $\Phi_0^a = \{P_0^a, V_0^a\}$. Then the first step of the demultiple technique is given by

$$\Phi_{pa} = \Phi_0 + a\Phi_{1a}, \quad (1)$$

where the inverse source signature is denoted by a , and Φ_{1a} is the multidimensional convolution of V_0^a by Φ_0 . See the illustration of events generated by the multidimensional convolution of V_0^a by Φ_0 in Fig. 2. Note that only free-surface multiples that have their first bounce in the subsurface above the BMG reflector are predicted and therefore attenuated. A second step is required to attenuate free-surface multiples that are still present in Φ_{pa} .

*E-mail: abiola25@yahoo.com

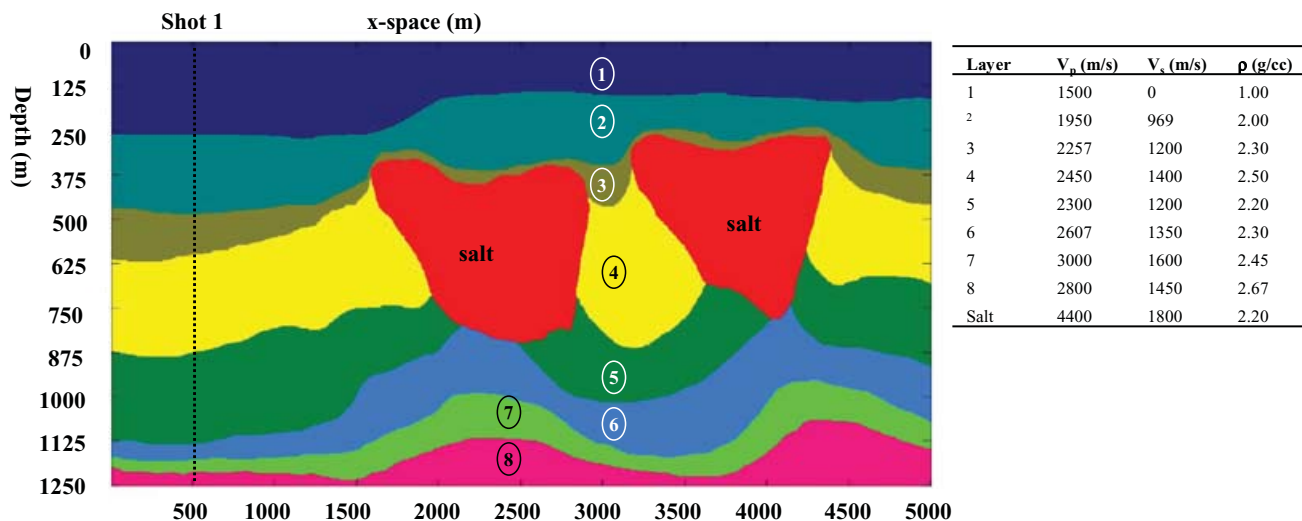


Figure 1 2D geological model adapted from Lafond *et al.* (2004). This is the geological model considered for the application of the BMG demultiple technique.

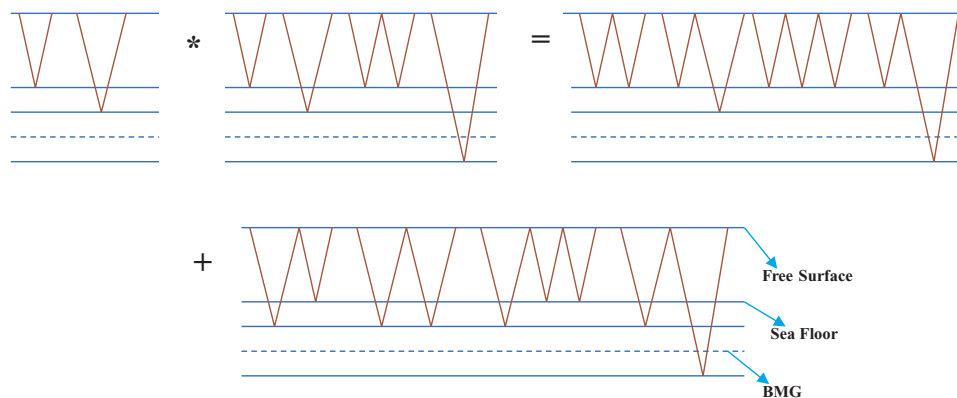


Figure 2 An illustration of the scattering diagram of free-surface multiples predicted by the multidimensional convolution of V_0^a by Φ_0 . These predicted free-surface multiples are attenuated using equation (1).

Let us denote V_{pa}^b as a portion of V_{pa} (V_{pa} is a component of Φ_{pa} corresponding to the particle velocity) located below the BMG reflector. The second step is given below as

$$\Phi_{pb} = \Phi_{pa} + a\Phi_{1b}, \tag{2}$$

where Φ_{1b} is the multidimensional convolution of V_{pa}^b by Φ_0^a . Figure 3 shows an illustration of events generated by the multidimensional convolution of V_{pa}^b by Φ_0^a . Note that the second step does not predict free-surface multiples whose first and last bounces in the subsurface are below the BMG reflector (see the scattering diagram illustrating these types of free-surface multiple in Fig. 4). These types of free-surface multiple are usually weak in deep water and therefore are as negligible as internal multiples.

Note that the advantage of the BMG demultiple technique described above, over other demultiple methods, which autoconvolve all the data, is that they are strictly based on the following series:

$$\Phi_p = \Phi_0 + a\Phi_{p1} + a^2\Phi_{p2} + a^3\Phi_{p3} + \dots, \tag{3}$$

where Φ_p denotes data without free-surface multiples, Φ_0 denotes the actual data containing primaries, multiples and ghosts, Φ_{p1} denotes the multidimensional convolution of Φ_0 by the vertical particle velocity (V_0), Φ_{p2} denotes the multidimensional convolution of Φ_1 by the vertical particle velocity (V_0), Φ_{p3} denotes the multidimensional convolution of Φ_2 by the vertical particle velocity (V_0), and so on. As described by Ikelle and Amundsen (2004), Φ_{p1} predicts all orders of

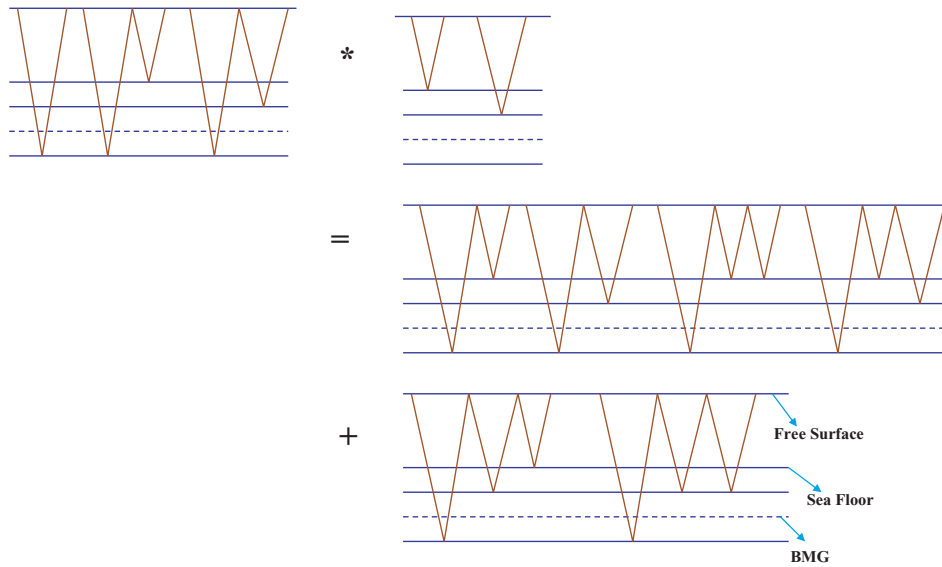


Figure 3 An illustration of the scattering diagram of free-surface multiples predicted by the multidimensional convolution of V_{pa}^b by Φ_0^a . These predicted free-surface multiples are attenuated using equation (2). Note that free-surface multiples that have their first and last bounces below the BMG reflector are not predicted.

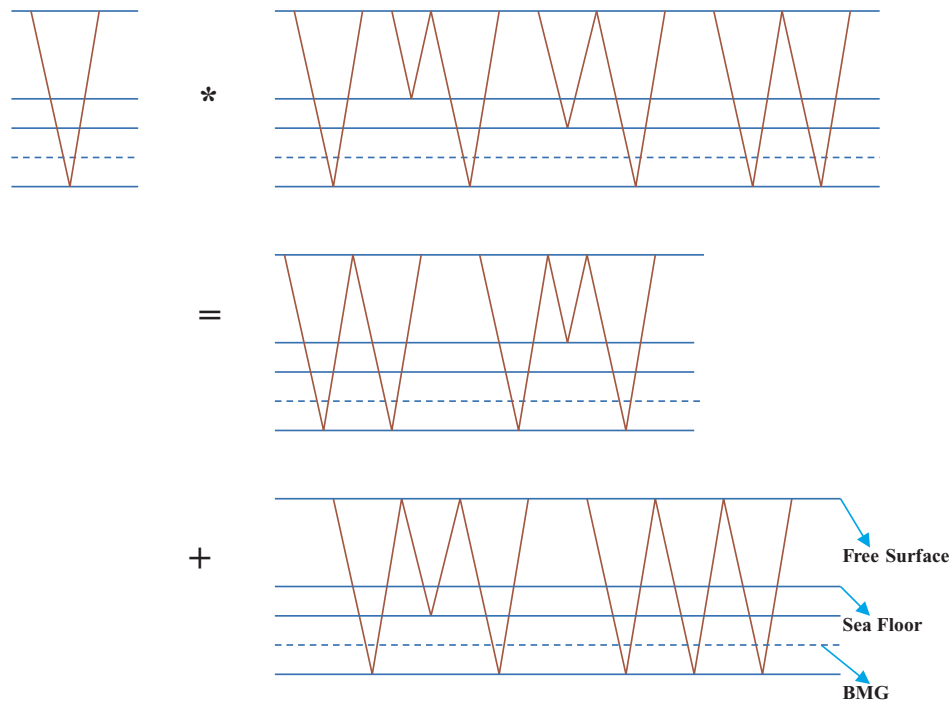


Figure 4 An illustration of the scattering diagram of free-surface multiples that have their first and last bounces below the BMG reflector and are not predicted in the two demultiple steps.

free-surface multiples. However, the amplitudes of the higher-order free-surface multiples included in Φ_{p1} are inconsistent with those of the actual data, Φ_0 . So, when using the demultiple technique which autoconvolves the whole data, we have

to include higher orders of the series in (3). Otherwise, by limiting the series in (3) to its first two terms, we will end up with significant residual multiples in our data, or we can end up distorting our primaries during the subtraction.

Having reviewed the demultiple technique of Ikelle *et al.* (2004), we now show that the technique will work even when the muting at the BMG reflector cuts through several seismic events of our synthetic data.

APPLICATION OF THE BMG DEMULTIPLE TECHNIQUE

We now examine the synthetic towed-streamer data used for our application, which we generated using the elastic finite-difference modelling technique. Figure 1 (adapted from Lafond *et al.* 2004) shows the 2D geological model considered for our application. We have designed our geological model to have a shallow water depth and irregular saltbodies that are located close to the sea-floor. Note that, due to the scaling down of our model (Fig. 1), the boundaries between materials in our model appear smooth; actually, they are rough. The multiple scattering below primaries and multiples (Fig. 5a) associated with the key boundaries of our model, like the sea-floor, are caused by the roughness of these boundaries.

We designed our geological model, as described above, in order to generate the primaries that are needed to predict multiples and to have their trajectories cross the BMG location. Our objective is to show the effectiveness of the BMG-based demultiple technique, even in this kind of situation. Therefore, we have generated 321 shots from 500 m to 4500 m (source depth 5 m), spaced at intervals of 12.5 m. The number of receivers used is 321; they are placed from 500 m to 4500 m (receiver depth 10 m) and spaced 12.5 m apart. We have based our analysis on a shot located at 500 m (Fig. 1 shows the location of the shot on the geological model while Fig. 5(a) shows a shot gather of the shot). We have considered this shot because it is a good representation of all offsets and events that pass through the saltbodies.

We now demonstrate the demultiple steps described in our introduction. We first defined the portion of the data containing only primaries V_0^a by muting the data at the BMG location. An example of V_0^a is shown in Fig. 5(b). We muted the data at the BMG location by taking a small portion of the actual data Φ_0 and performing the autoconvolution of this small portion to produce a portion of Φ_1 containing the first multiples that we needed to define the BMG location. Note that from the example shown in Fig. 5(b), V_0^a is small in comparison with the actual data (Fig. 5a). Note also that the mute at the BMG location cuts up the primary of the top of the saltbody.

We now examine the multiples predicted by the multidimensional convolution of V_0^a with the actual data Φ_0 . The result of the multidimensional convolution is denoted here as Φ_{1a}

(an example is shown in Fig. 5c). The multiples contained in Φ_{1a} are predicted free-surface multiples whose first bounce in the subsurface is located above the BMG reflector. Note that the multiple of the primary of the top salt that was cut-up at the BMG location in Fig. 5(b) is not predicted fully.

When comparing the field of predicted free-surface multiples in Fig. 5(c) with the actual data in Fig. 5(a), it should be remembered that the field of predicted free-surface multiples in Fig. 5(c) corresponds to Φ_{1a} ; it has not been scaled by the inverse source signature a . In other words, the apparent wavelet of multiples contained in the field of predicted free-surface multiples is different from the apparent wavelet of multiples contained in the data. This remark applies throughout the paper to all the comparisons between multiples and the multiples in the actual data.

The next step is to apply (1) to attenuate multiples predicted in Φ_{1a} . The demultiple result Φ_{pa} after step one is shown in Fig. 5(d). Note that free-surface multiples which are not predicted by Φ_{1a} are still present in Φ_{pa} . We have applied the second step, described by (2), of the demultiple technique to attenuate the remaining free-surface multiples.

We first compute the portion of the Φ_{pa} below the BMG, V_{pa}^b . An example of V_{pa}^b is shown in Fig. 6(a). The multidimensional convolution of V_{pa}^b with the portion of the actual data above the BMG reflector, Φ_0^a , predicts Φ_{1b} (Fig. 6b). The multiples contained in Φ_{1b} are free-surface multiples which have their first bounce below the BMG reflector. Note in Fig. 6(b) that the other portion of the multiple associated with the cut-up primary of the top of salt is predicted. Using (2), the final demultiple result Φ_{pb} (Fig. 6c) is obtained. Note in Fig. 6(c) that the free-surface multiples interfering with primaries at about 0.7 s to 1.22 s have been strongly attenuated.

It should be noted that the BMG should not be shallow, and if it is shallow, it has to be lowered, according to Ikelle *et al.* (2004). For this demonstration we have made our BMG location shallow so that we can obtain primaries that severely overlap the BMG location.

We have also included the zero-offset data before and after the demultiple to aid our analysis further. Figure 7(a) shows the zero-offset data before demultiple. Note that the interference of free-surface multiples with the primaries is common in the section. We have pointed out three examples of such interference. Figure 7(b) shows the zero-offset data, after applying the second step of the BMG demultiple. Note that the free-surface multiples have been attenuated and that the mute at the BMG location, which cuts across

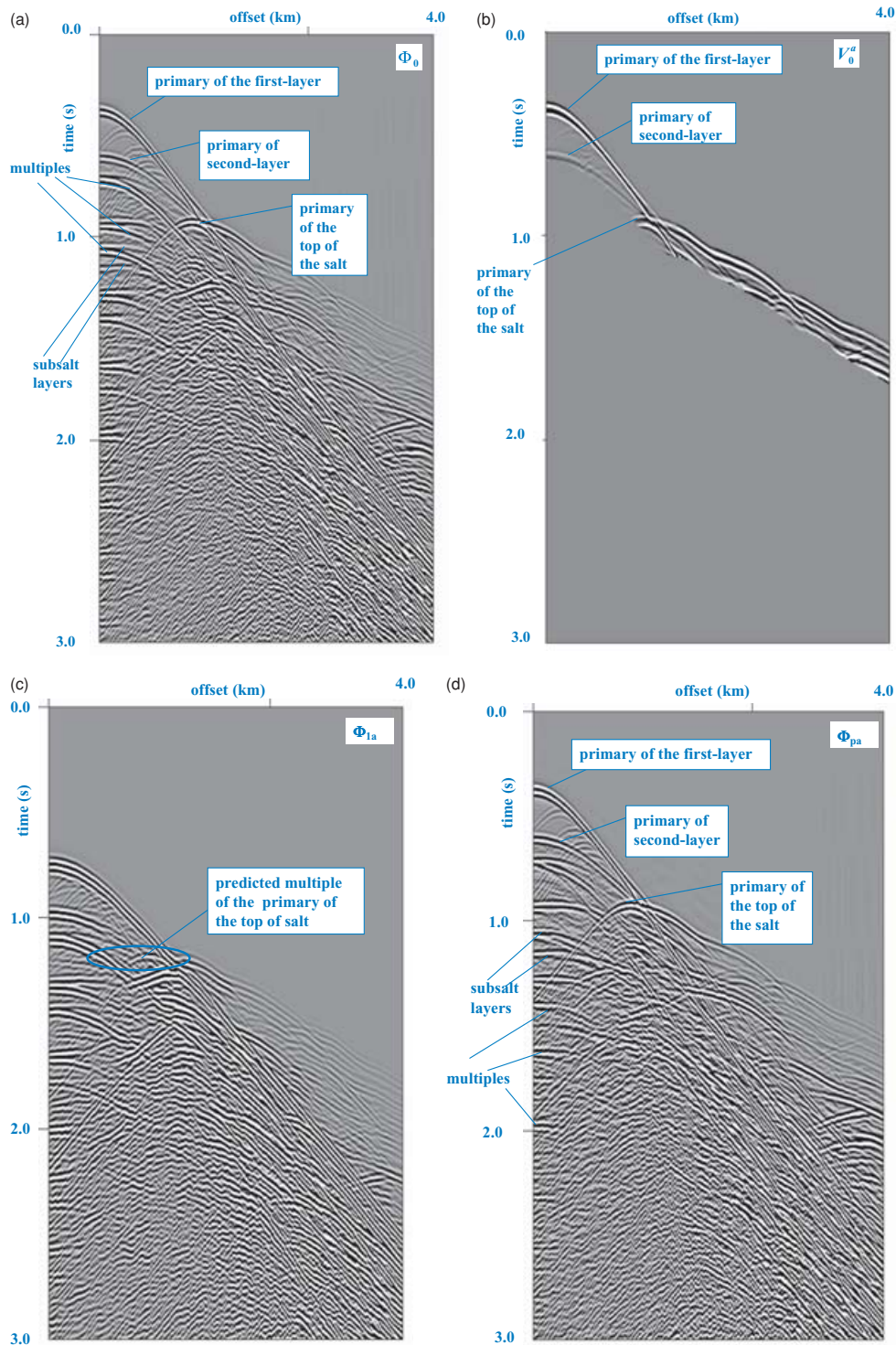


Figure 5 (a) Shot gather of the shot located at 500 m generated from the geological model in Fig. 1 (this is an example of the actual data Φ_0). Note that free-surface multiples interfere with primaries at about 0.7 s to 1.22 s. (b) An example of V_0^a (the portion of the particle velocity of the data containing only primaries located above the BMG reflector). Note that the mute at the BMG location cuts up the primary of the top of salt. (c) An example of predicted multiples Φ_{1a} . Note that the multiple of the primary of the top of salt cut up by the BMG is not predicted fully. (d) The result of the demultiple after applying equation (1). Note that Fig. 5(d) contains some free-surface multiples which are not predicted by Φ_{1a} . We applied the second step of the demultiple technique described in equation (2) to attenuate these free-surface multiples.

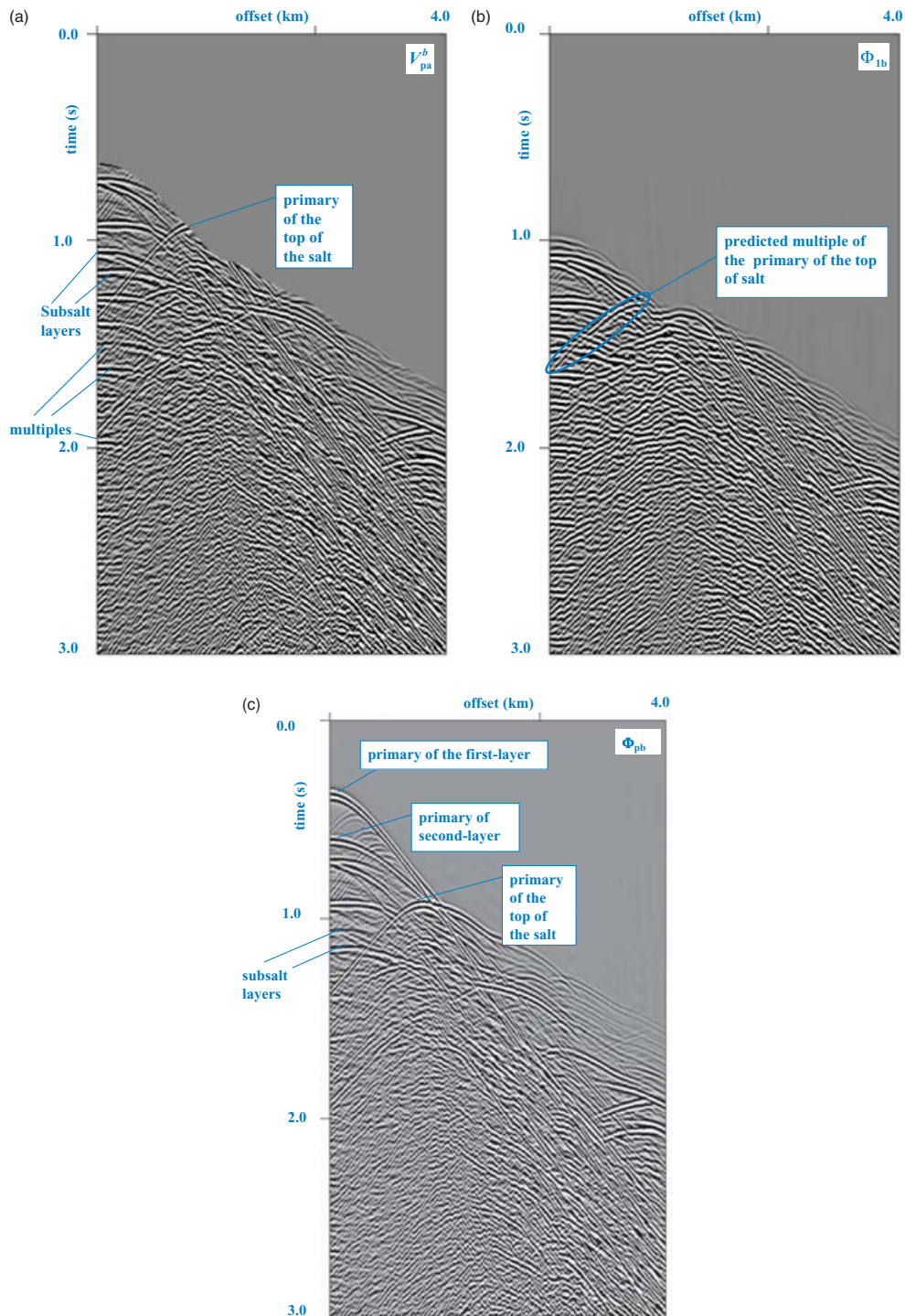


Figure 6 (a) An example of V_{pa}^b (the portion of the particle velocity of Φ_{pa} located below the BMG reflector). (b) An example of predicted free-surface multiples Φ_{1b} . Note that the other portion of the multiple of the primary of the top of salt cut up at the BMG is predicted. (c) The final demultiple result obtained after applying equation (2). Note that most of the free-surface multiples that interfere with the primaries at about 0.7 s to 1.22 s have been attenuated. The free-surface multiples that are still present in the final demultiple result are those not predicted in both steps of the demultiple technique. (Figure 4 shows an illustration of these types of free-surface multiples.) Note that because we have made our water depth shallow for this demonstration of the BMG demultiple technique, the leftover multiples are visible. Ideally, in deep water, which is usually the case in marine acquisition, these multiples will appear weak and therefore negligible.

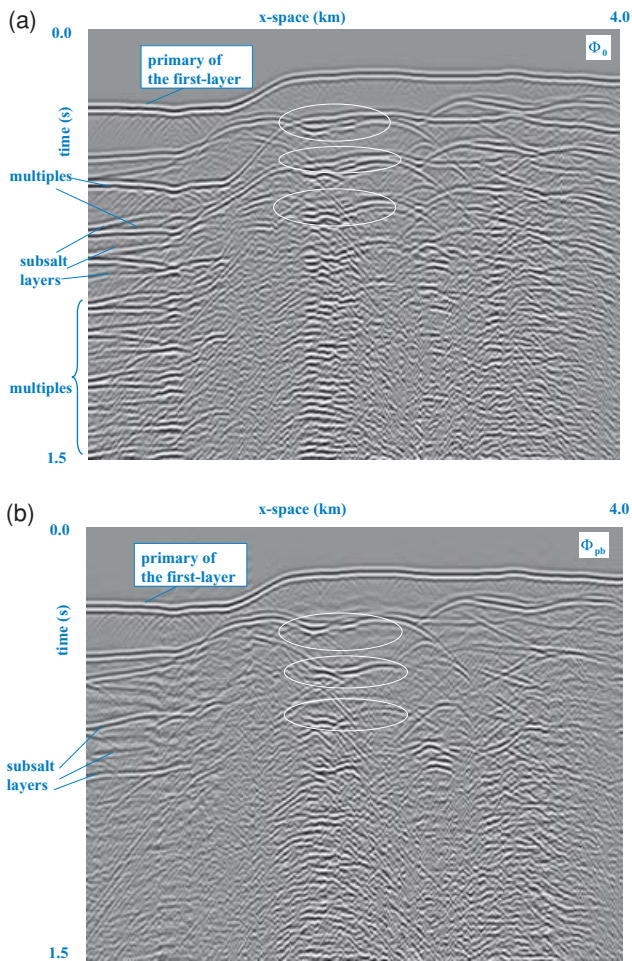


Figure 7 (a) Zero-offset data before the demultiple. Note the interferences of free-surface multiples with primaries; The circled area in the figure indicates examples of such interferences. (b) Zero-offset data after applying the second step of the BMG demultiple technique. Note that the free-surface multiples have been attenuated. From this final demultiple result we show that the mute at the BMG location, which cuts across several seismic events, does not affect the accuracy of the demultiple. Note also, that the weak primaries of the subsalt layers can be traced along the section as compared to the zero-offset data before the demultiple in Fig. 7(a)

the primaries, did not affect our final result. Also note that the weak primaries of the subsalt layers can be traced along the section, as compared to the zero-offset data before the demultiple.

CONCLUSION

We have demonstrated numerically that the BMG demultiple technique is effective and not sensitive to the way the mute at the BMG location is applied. Even when the mute at the BMG cuts through several seismic events, it does not affect the demultiple result. Therefore we conclude that the BMG is applicable in both complex geology and long-offset data.

ACKNOWLEDGMENTS

We thank the sponsors of the CASP project for their comments and suggestions during the review process. We also thank the reviewers of this paper for their constructive comments.

REFERENCES

- Ikelle L.T. and Amundsen L. 2004. Attenuating primaries and free-surface multiples of towed streamer data while preserving ghosts of primaries: a linear approach. *Journal of Seismic Exploration* **13**, 1–15.
- Ikelle L.T., Osen A., Amundsen L. and Shen Y. 2004. Noniterative multiple-attenuation methods: linear inverse solutions to nonlinear inverse problems II – BMG approximation. *Geophysical Journal International* **159**, 923–930.
- Lafond J.I., Bridson M., Houllevigue H., Kedran Y. and Peliganga J. 2004. Challenges in deep offshore imaging: West Africa. CSEG National Convention, Calgary, Canada, Expanded Abstracts.